

7th QUARTERLY PROGRESS REPORT

Submitted to

NATIONAL AERONAUTICS & SPACE ADMINISTRATION

Manned Space Flight Center

Houston, Texas.

FACILITY FORM 602  
N 66-80235  
(ACCESSION NUMBER)  
33  
(PAGES)  
QR-65070  
(NASA CR OR TMX OR AD NUMBER)

(THRU)  
None  
(CODE)  
(CATEGORY)

by

SOLID STATE RADIATIONS INC.

2261 S.Carmelina Avenue

Los Angeles 64, California

Contract No. NASw-415

January 1964

## FOREWORD

During the previous six quarters of work on the contract, the emphasis has been directed toward the development and application of semiconductor detectors to invivo measurements of radiation. The results of this work can be summarized as follows:-

- (1) Development of fabrication techniques for 3mm diameter and 1mm diameter diffused junction detectors hermetically sealed into the end of flexible cables. These units are characterized by thin ( $< 2$  micron) entrance windows, and shallow depletion depths ( $\sim 100$  microns) making them useful for invivo detection of  $\alpha$  particles, low energy protons and  $\beta$ -rays. Their  $\gamma$ -ray sensitivity is low.
- (2) The development of a PIN lithium ion drift detector packaged in a similar manner. The PIN lithium ion drift detectors are completely depleted and have heavy ( $\sim 10$  mils steel) entrance windows. They are useful for energetic  $\beta$ -rays and have small but usable efficiency for  $\gamma$ -rays, about 2%.
- (3) The packaging of a low noise muvistor-transistor hybrid preamplifier suitable for use in medical settings. A companion power supply was also developed.
- (4) The fabrication of the invivo detectors in the form of slender rigid probes of rugged construction for surgical use.
- (5) The development of a preamplifier in the form of a probe handle which can be sterilized for surgical use.
- (6) The development of a threshold discriminator and count rate circuit for application of the probes to surgical procedures.
- (7) Experimental evaluation and application of the probes to a variety of problems in clinical medicine.

At the conclusion of the sixth quarter of work, the objective of the contract was redirected toward applying the technique developed previously to the development of dosimetry techniques for use in conjunction with the manned space program and more specifically, the Apollo program.

This effort falls roughly into three tasks: (1) a study of the biological hazards associated with the mission; (2) the evaluation of a dose measuring approach, which can assess this hazard; and (3) the development of a prototype instrument based on these principles. The work covered by this report represents the completion of these tasks culminating in the delivery of a laboratory model of a space dosimeter.

## I. INTRODUCTION

To ensure the successful completion of the Apollo mission, it is necessary to assess the biological hazards of human bodies due to ionizing radiation in space. The conventional means of dose measurement present a number of serious limitations. Most medical procedures, for which the majority of radiation dose measuring instruments have been calibrated, involve the use of photons or very high energy  $\beta$  particles. However, some of the most severe radiation hazards in the Apollo mission are in connection with heavier charged particles such as protons. For this reason, a direct application of radiation dose instruments and data from the medical field is difficult. Other difficulties arise from the fact that dose rate can vary over very large ranges. Because of the long duration of the proposed space missions, a dose rate threshold in an instrument would be very undesirable, since it may be anticipated that a relatively low dose rate will be encountered over a substantial part of the mission but with significant accumulated dose. During passage through trapped radiation and in the presence of solar flares, the dose rate can climb to very high levels for short periods of time. Under these conditions, any saturation effects would, of course, be undesirable. Among various requirements for space instrumentation is the continuous availability of readout of accumulated dose and dose rate in order for the astronaut to assess the radiation hazard status of the mission and thus be able to make operational decisions concerning it. However, the permanent nondestructive record of the radiation history of the mission is likewise of great interest.

In the past, radiation dose measuring instruments have been primarily of two basic types: air ionization chambers and chemical dosimeters. The air ionization chamber represents the standard by which

other instruments are usually calibrated, but has the drawbacks of low sensitivity, difficulty of readout and poor retention of information for long periods of time due to leakage. Chemical dosimeters which include such things as photographic films, thermoluminescent and fluorescent glass dosimeters basically utilize physical and chemical changes which occur more or less reversibly. These dosimeters have the advantage in many cases of their capacity to accumulate dose with minimum threshold effects and retain this information for long periods of time. However, they do not generally provide dose rate information and are generally available for readout only on a destructive basis, i.e. one which erases previous information.

The silicon semiconductor nuclear particle detector has many interesting properties which lead to its potential application to these problems. It is essentially a solid state ionization chamber having many of the properties of a gas chamber with the notable exception of the higher density of the ionizable sensitive volume. For this higher density many advantages and some disadvantages accrue. Among the advantages are much higher sensitivity to small volumes, a better approximation to tissue for certain types of radiation and a physical ruggedness rendering it suitable for space vehicle use. Its disadvantages stem from the inherent leakage currents associated with semiconductor junction devices and the resulting electronic noise which tends to obscure low energy radiation events. In order to take advantage of the useful properties of these detectors and circumvent difficulties, a number of novel circuit approaches have been devised. These consist of coupling the good efficiency and response of the semiconductor detector to the long term memory of electrochemical integrators. Recent developments in the latter field have made possible the accumulation of charge virtually without threshold up to large values although at the same time providing nondestructive readout of the recorded information. The teaming of these two devices with suitable circuitry, makes possible personal dosimetry packages having a volume of 2 cu.in. or less including the selfcontained power supply. This makes possible the location of dosimeter packages on the body of the astronaut with minimum discomfort and interference with normal functions. This latter property is of great

importance since calculations would appear to indicate that dose can vary considerably from one point to the other in space capsules and that reliable dose information is best obtained from dosimeters in intimate contact with personnel.

## II. DOSIMETRY PROBLEM - DEFINITION OF TERMS

A number of terms are in use in the health physics field which must be carefully defined in order to ensure that various workers can meaningfully compare data. The biological significant effects of radiation are extremely complicated, and error in the definition of terms can lead to severe discrepancy in assessing the biological hazard from radiation. The unit of radiation which was recommended and adopted by the International Commission on Biological Units at the 7th International Congress of Radiology 1953 is the RAD. This is defined as the unit of absorbed dose which is 100 ergs per gram in any medium. The RAD is a measure of the energy imparted to matter by ionizing radiation per unit mass of irradiated material at the place of interest. For dosimetry purposes, this unit has displaced the original unit of X-ray or  $\gamma$ -ray dosage, the roentgen, which was defined in terms of the ionization produced in air and the roentgen equivalent physical (REP) which related this unit to the radiation dose in tissue. The RAD is a precise physical unit, but does not give the entire story concerning the biological effect of radiation. For this purpose, the Roentgen Equivalent Man or REM, has been used to express human biological dose as a result of exposure to one or many types of ionization radiation. The dose in REMS is equal to the absorbed dose in RADS times the relative biological effectiveness (RBE) factor of the type of radiation being absorbed. The RBE factor is then the significant factor in comparing the biological effect of radiation dosage from a given type of radiation to that of X-rays or  $\gamma$ -rays; it is the ratio of the number of RADS of X-rays or  $\gamma$ -rays to the number of RADS of the other radiation which produce the identical effect on experimental organism or tissue. Since the effect of radiation on various parts of the human body is extremely variable, a number of terms are important in assessing the radiation hazards. The

skin dose represents the sum of air dose, back scattering and possibly exit dose from other parts if this is significant. It represents the energy deposited in approximately 1mm of tissue but in the case of heavily ionizing particles should exclude the dose deposited in the 100 microns or more of epidermis. Depth dose refers to that dose delivered at a particular depth beneath the surface of the body and usually includes the dose to various deep lying radiation sensitive organs such as the bone marrow and viscera. Eye dose represents the dose to the cornea of the eye which has been shown to be particularly radiation sensitive with the induction of radiation cataracts by relatively small dosage. This represents a specialized location for skin dose, the significant depth being in the 1mm region. By dose threshold in both the organism and in instruments, one means the minimum dose that will produce a detectable degree of any given effect.

### III. RESPONSE OF SILICON DETECTORS

As was stated in Section I, the silicon detector can be considered as a solid state ionization chamber in which every 3.5 electron volt produces one hole-electron pair, of  $1.6 \times 10^{-19}$  coulombs, of collected charge. This figure has been shown to be constant for all types of particles from minimum ionizing electrons to heavy multiple charged nuclei. It is the extreme linearity of collector charge with energy losses that provides the most interesting properties of the detector for dosimetry purposes. The response to photons of course, is dependent on the mode of interaction between the photon and the silicon crystal. These interactions are different for differences in energy in the photon and for this reason become rather complicated. The atomic number of silicon is 14 as contrasted with 8 and 1 for oxygen and hydrogen, the principal constituents of tissue and for this reason its response is quite different from that of tissue. At high energies the response to  $\gamma$ -rays is almost completely the result of Compton interactions. As the energy falls to 100 Kev and lower, there is an increasingly greater number of photoelectric processes in which the entire photon energy is imparted to an electron. This results in a somewhat peaked response in the 100 Kev photon range.

The interaction with high energy protons however, is much simpler and is described almost completely by the mass absorption.

By mass absorption, one means that the loss of energy for a proton is related rather simply to the mass of material through which it passes. More precisely, it is characterized by  $\rho Z/A$ . For this reason, the stopping power of materials of different atomic numbers can be compared by factors which are independent of proton energy. In short, the energy absorbed from a proton flux by a gram of silicon is related to that absorbed by a gram of tissue, by a simple numerical factor. The problem then, of measuring dose, is resolved into one of measuring the total energy deposited in a detector of known mass. This energy will be manifest as a series of current pulses resulting from the interaction of individual protons with the silicon crystal. These interactions range from total absorption at low energies to the deposition of a charge equivalent to approximately 0.4 Mev/mm of path in the detector, for very high energy protons, which are essentially minimum ionizing. A description then, of the detector response will require a knowledge of the anticipated spectrum.

#### IV. DESCRIPTION OF THE PROTON FLUX

Measurements of protons in space have shown a large variation in the spectral composition depending on altitude, geomagnetic latitude and state of solar activity. However, all these spectra have several factors in common. The protons are increasingly abundant at successively lower energy, the observations on the low energy end being limited by the cut-off of the observing instruments. As the energy increases, the distribution falls monotonically to quite low values at energies in excess of 1 Bev. These extremely high energy particles are quite penetrating and hence, are not degraded appreciably in the structure of the spacecraft. Their total contribution to dose is quite small. On the low energy end of the scale, the protons will be stopped either in the skin of the spacecraft or in the course of penetrating various interior structures. Since the range of 30 Mev protons is approximately 5mm in aluminum, there should be little contribution to dose at energies below this order of magnitude. The most damaging protons are those which are degraded in the spacecraft to an energy where they are intensely ionizing in tissue. Anticipating the dose

rate then is extremely difficult, since it will depend on a very detailed description of the middle range of the spectrum and the precise amount of degrading materials at critical locations. This points up the difficulty of measuring dose in an actual operational situation. Energetic protons become more and more severely damaging as they slow down, and the amount of slowing down depends on the quantity of degrading material, which in turn affects the cut-off for low energies. Ideally, the measurement of dose would take place at the actual sites of biological damage. This is, however, not possible, even with in-vivo dosimeter techniques. The best approximation would be the measurement of the dose rate at the surface of the astronaut's body with a dosimeter shielded to degrade the incident particles to the energy distribution which they would have after penetrating an appropriate depth of tissue. It is useful to look at the typical distribution of pulse heights that might be encountered in such a detector. The extremely high energy protons are hardly degraded at all. Above 1 Bev the protons are hardly distinguishable from other minimum ionizing particles. These, at any rate, are few in number, and ignoring the dose produced would hardly introduce a serious error. At energies between 250 Mev and 500 Mev, the energy deposited per unit length begins to climb to the point where it becomes a serious source of dose; but there, the silicon is still rather transparent. Pulses corresponding to two to three Mev per millimeter characterize this region with little degradation even from as much as 10cm of equivalent tissue degrader. In the vicinity of 100 Mev, the depth dose problem becomes increasingly serious. These protons are sufficiently energetic to penetrate the spacecraft and several centimeters of tissue at which point they are very intensely ionizing as they come to the end of their range. If the end of the range is the detector, then the signals will be of the order of 10 Mev/mm. With proton energy below 100 Mev, the signals will be increasingly large until the threshold of detection is reached. This is the energy which barely permits a proton to reach the detector through the degrader. At this point, pulse heights decline rapidly from a maximum to zero.

## V. SURFACE AND EYE DOSE

Special consideration should be given to that portion of the spectrum which is neglected in depth dose considerations. The cornea of the eye is particularly radiation sensitive. Many of the early workers with charged particle beams suffered radiation cataracts as a result of their failing to appreciate this problem. In this case, protons with a range of less than 1mm of tissue must be considered. This corresponds to the range of a few Mev, and is most likely to result from almost totally degraded protons as well as secondary protons from nuclear scattering and reactions. To detect these radiations, a silicon detector without degrader or appreciable entrance window would be used. The pulse heights of interest would range from about 0.5 to 5.0 Mev in a thin, say 100 micron detector. The high energy portion results from other than normal incidence. The eye dosimeter, even more than the depth dose instruments, needs to be located as close as possible to the actual sensitive site. A simple compact instrument would greatly aid this.

## VI. ESTIMATION OF THE ORDERS OF MAGNITUDE

The most intense solar flare reported would produce a dose of less than 100 R/hr. This figure is then a convenient upper limit for the dose rate. At the opposite end of the scale there is little use in considering rates much less than  $10^{-4}$  R/hr, since this is of the order of terrestrial background dose. As far as total dose is concerned, a dose of 1000R is almost invariably fatal if not totally debilitating, and for practical reasons is about the maximum dose to be considered. Instruments however, should not produce gross errors if subjected to greater dose than this. In other words, dose of 1000R or greater should never indicate less than 1000R due to saturation effects. A total accumulated dose of 1R is probably negligible for a mission. However, increments of dose of down to 1% of this value might be of interest in tracing dose build up conditions, so should be detectable. Using this data, and the previous discussion of the spectrum, it is instructive to compute the requirements of a dosimeter package.

Since

$$1 \text{ Rad} = 100 \text{ ergs/gm} = 10^{-5} \text{ joules/gm} = 6 \times 10^7 \text{ Mev/gm}$$

and in tissue the  $dE/dx$  for a proton of say 30 Mev is about 15 Mev/gm, then

$$1 \text{ Rad} = 4 \times 10^6; \text{ 30 Mev protons for the peak dose rate of 100 Rad/hr.}$$

$$100 \text{ Rad/hr} = \frac{4 \times 10^8}{3600} = 1.12 \times 10^5; \text{ 30 Mev protons/cm}^2/\text{sec.}$$

This is well within the capacity of ordinary pulse technique, since for a typical detector the area is of the order of  $0.04 \text{ cm}^2$ . Thus, dose rate is no problem, even for rates ten times as great or proton energies ten times as high.

## VII. SYSTEM DESIGN CONSIDERATIONS

Every dosimeter system can be reduced to two elementary processes. These are (1) the conversion of absorbed energy to electron-ion (or hole) pairs in the absorbing medium; and (2) the recording or accumulation of these charges to constitute an observable quantity. In some cases, such as with dosimetry ion chambers, the two processes are combined into one device, the gas contained in the chamber accomplishing (1) the deflection of a quartz fiber electrometer accomplishing (2). In other cases, a number of intermediate steps are imposed. For example, in thermoluminescent dosimetry (1) takes place in the  $\text{CaF}_2$  crystal. The results are stored as excited states of the crystal. Heating produces the emission of light which ejects photoelectrons from a photocathode which are amplified by electron multiplication. These in turn actuate an integrator for (2). In the case of the silicon semiconductor dosimeter (1) is accomplished by the dissipation of energy in a silicon crystal representing the generation of hole-electron pairs. It is useful to estimate the yield for this process.

Lithium ion drift detectors have been fabricated with sizes ranging from  $1 \text{ cm}^3$  to  $.001 \text{ cm}^3$ . A spherical geometry is clearly desirable from the point of view of lack of directional discrimination. This shape does not lend itself to simple attachment of collecting electrodes so a cubic approximation is used. If a  $1 \text{ cm}^3$  detector were used, difficulties would be encountered from two sources. First, collection of carriers from such a deep counter would require high voltages or low temperatures, both

of which are inconvenient in a dosimeter. Second, the counter would be thick compared with the range of significant energy particles leading to departure from behavior as a Bragg-Gray cavity. Detectors much smaller than 1mm on edge are difficult to fabricate, and at any rate would have vanishing response. From these considerations, a 2x2x2mm cube is considered as a good size for the detector. The volume is then

$$(0.2)^3 \text{ cm}^3 = 8 \times 10^{-3} \text{ cm}^3$$

At a density of about  $2.3 \text{ gm cm}^3$ , this gives a mass of

$$M = 1.8 \times 10^{-2} \text{ gm}$$

One Rad then deposits 1.8 ergs in the detector, or

$$1 \text{ Rad} = 1.8 \times 10^{-7} \text{ joules/detector.}$$

The charge yield in coulombs is this number divided by 3.5ev since ev x coulombs gives energy, or

$$1 \text{ Rad} = \frac{1.8 \times 10^{-7}}{3.5 \text{ ev}}; = 5 \times 10^{-8} \text{ coulombs.}$$

This is an appreciable charge. If there were no leakage a chamber of 100pf capacitance would charge to a voltage of 500 volts, but unfortunately, it is difficult to reduce the leakage of such devices, even with guard rings, to less than  $10^{-7}$  amperes due to thermally excited carriers. This would be equivalent to 1 Rad per minute and thus obscure any lesser dose rate. For this reason, the integration and observation of the DC current resulting from the collection of this charge cannot be used even though its simplicity has great attractions. Instead, the individual pulses will be utilized, since the pulse-like nature of the individual proton-detector interaction provides an ideal means of discriminating against the background leakage current.

As we have seen earlier, the range of magnitudes of pulses will be from about 1.5 Mev (three times minimum ionizing) at 250 Mev incident energy, to 20 Mev, the energy lost by a particle that just stops in the 2mm depth of the detector. Noise, due to leakage current and

electronic limitations is of the order of 30 Kev FWHM. Minimum ionizing particles deposit about 0.8 Mev. If neither of these sources of background are to influence the dose measurement, a threshold for response should be set at some higher figure, of the order of 1 Mev. Thus, amplification to bring the detector signals up to a level which permits setting a threshold electronically at about 1 Mev is required. This sets the minimum required gain of the amplifier system. The maximum gain that can be tolerated is limited by the linear output range of an amplifier; about 10 volts for low power transistor circuits. This would call for a charge sensitivity of about 0.5 volts per Mev producing a range of signals from 1 to 10 volts.

#### VIII. DEGRADER CONSIDERATIONS

For a depth dose measurement it is necessary to degrade the proton flux to simulate the spectrum at depth. Degradation by tissue equivalent material would be extremely cumbersome, requiring a sphere of approximately 20cm diameter to get a good depth dose simulation. Fortunately, only a few millimeters of tissue equivalent material need be in contact with the detector, since the range of secondaries from protons is small. The balance of the degrader can be any dense material such as tungsten, gold or lead. These mass absorbers degrade the proton spectrum in proportion to their density, so for a density of 16, only 6mm of degrader are needed for a 10cm tissue depth. Such a shell has a very small mass and should not prove cumbersome.

For the surface/eye dose no degrader is used. To simplify the electronics, the same mass detector is used. If the depletion depth is 0.01cm as would be the case for a diffused junction, then an area of  $0.8\text{cm}^2$  is required or a circular detector of roughly 1cm diameter. This is a good approximation to the sensitive area of the eye.

#### IX. STORAGE OF DATA

The detector and associated amplifier produce a pulsed signal having rise and decay times of the order of a microsecond. We must now consider means for accumulating this data. If only laboratory use were

contemplated, a multi channel pulse height analyzer would be the ideal tool for the accumulation of data. This would store the number of pulses having a given amplitude for a hundred or more discrete amplitudes. However, this information is quite redundant since the distribution is  $F(E)$  then the dose is clearly

$$D = \int_{\text{threshold}}^{\infty} hF(h)dh$$

Some form of pulse integrator can be used, and the complexity of pulse height analysis can be eliminated. In the choice of an integrator, the actual operational considerations are primary. Some of these are as follows:

- (1) High reliability and proof against loss of data.
- (2) Small size and weight for high capacity.
- (3) Zero or small standby power consumption.
- (4) Absence of aging, drift, or threshold effects.
- (5) Simple, precise readout.

These are met by the use of a device, extremely old in principle, but only recently developed for practical use. This is the electrochemical cell, or shorter, the E-cell. In the E-cell, an electric current is passed from a metallic electrode through an electrolyte of a salt of this metal to a neutral electrode. Faraday's law states that the mass of metal transferred is one chemical equivalent for every 96,500 coulombs of charge which is passed. The precision of this relationship is such that, until recently, the standard ampere was defined in terms of the weight of silver plated in a cell when a current of one ampere was passed for one second. These devices have been available from several manufacturers. One of the most convenient is a silver cell manufactured by the Bissett-Berman Company of Santa Monica, California. This is a three electrode cell in which the readout is accomplished by transferring the plated silver to a third electrode and recording the charge necessary to reach a reaction end point. Since the metal is held on the third electrode, readout is essentially nondestructive, since the information may be obtained by back plating any number of times. A second is the Solion cell manufactured by Self-Organizing Systems Inc. of Dallas, Texas. This is an iodine cell

in which iodine is plated through a semipermeable membrane in a three compartment cell. It provides the interesting feature of continuous readout of the integrated quantity without interruption of the readout cycle. The threshold for both of these devices is about  $10^{-5}$  coulombs. That is to say, that a charge of this magnitude produces a clearly defined readout. In terms of rate of accumulation, both are effectively free of threshold, being able to integrate currents in the pico-ampere region. The use of these cells requires that the pulsed voltage signals be converted back to charge signals of the same type that occurred in the detector, but with enhanced amplitude and free of background. An inverse of the charge amplifier is required together with an electronic switch which opens the integrator circuit except when a pulse exceeding the pre-set energy threshold is present. If 10 microcoulombs is to correspond to the minimum dose of interest, about  $10^{-2}$  Rad, then the conversion constant of the complete system can be specified

$$1 \text{ Rad} = 10^{-3} \text{ coulombs}$$

At the detector

$$1 \text{ Rad} = 5 \times 10^{-8} \text{ coulombs}$$

Thus the charge gain on the complete system is

$$\frac{10^{-3}}{5 \times 10^{-8}} = 2 \times 10^4$$

The charge gain is just the charge to voltage gain of the charge sensitive amplifier times the voltage to charge gain of the voltage to charge converter. The former is

$$\frac{0.5 \text{ volts/Mev} \times 315 \times 10^{-6} \text{ Mev/h-e pair}}{1.6 \times 10^{-19} \text{ coulombs/h-e pair}} = 1 \times 10^{13} \text{ volts/coulomb.}$$

The latter must be  $0.5 \times 10^{-9}$  coulombs/volt. This has the dimensions of a capacitance, and as we shall see this is an actual capacitance used to make the conversion.

X. DETAILED DESIGN OF THE SYSTEM

1. Detector - As was discussed in the previous design considerations, the detector is a 2x2x2mm lithium ion drift detector. The detector is prepared by the conventional method of diffusing lithium into one face of a p-type silicon wafer and then subjecting the wafer to an electric field at elevated temperatures. Under the influence of the electric field, the lithium donors are distributed throughout the crystal lattice in such a way as to compensate the acceptor centers in the wafer. The result is a completely depleted PIN structure in which the n contact is formed by the lithium diffusion, the p contact by the uncompensated base material and the intrinsic layer by the compensated material. To guard against the possibility of further drift under elevated temperature conditions, sufficient undepleted silicon is left at the rear of the wafer to permit drift to take place. The wafer is diced into 2x2mm sections which are etched and mounted in standard TO5 transistor cans. The can is filled with a silicone rubber which serves the dual role of protecting the junction against contamination and providing a matrix of tissue equivalent material to improve the response of the dosimeter. The transistor can is welded shut to a standard 3-wire header. This is a convenient shape for inserting in a degrader shield and for plugging into the preamplifier. When operated into a conventional test facility using clipping time constants of 1 microsecond, the detectors exhibit a noise level between 30 and 20 kilovolts FWHM.
2. Amplifier - The amplifier employed is an all transistor lowpower consumption amplifier developed under NASA Contract NASw-383, (Fig.5) used in connection with space physics experimentation by the Jet Propulsion Laboratory. The principal requirement for this amplifier is stable low noise operation with a minimum of power consumption. Because of the latter requirement, the nuvistor hybrid preamplifier developed earlier in the course of the contract could not be employed, since the nuvistor requires approximately 1 watt of power for its operation.

The contribution of an individual noise source to the noise output of a detector-amplifier system involves the integration over frequency of the product of the noise  $n(\omega)$  and amplifier gain  $g(\omega)$ .

The gain  $g(\omega)$  depends upon the pulse shaping network of the amplifier. The simplest network, which is one of the best from a noise viewpoint, is an amplifier containing one  $R_1C_1$  integrator and one  $R_2C_2$  differentiator, the two time constants being equal. For such an amplifier  $g(\omega) = \omega\tau / (1 + \omega^2\tau^2)$ , where  $\tau = R_1C_1 = R_2C_2$  and  $\omega = 2\pi f$ . If a nuclear particle deposits a charge  $Q$  on to the input capacitance  $C$  in a time which is short compared to  $\tau$ , the amplifier will pass an exponentially rising and falling pulse with a maximum height equal to  $0.37 Q/C$  independent of  $\tau$ . The discussions which follow refer to such an amplifier.

Analogous to the situation found in detector-vacuum tube amplifier systems, a study of noise in detector-transistor amplifier systems, indicates that there are only two important noise sources to consider. One source has its origin in the input transistor base current and detector leakage current, and the other is related to the collector current.

The base and detector leakage current noise source may be represented by a white noise current generator at the amplifier input with a magnitude of  $i_{rms}^2 = eI_{in} \int \omega / \pi$ , where  $e$  is the electronic charge,  $\int \omega$  is the frequency interval and  $I_{in} = I_b + I_d$  is the sum of the base and detector currents. Since this generator is shunted by the total input capacitance  $C$ , the rms noise voltage squared per unit bandwidth, (referred to the amplifier input) is equal to  $(eI_{in}) / (\pi \omega^2 C^2)$ . The integration over frequency obtains

$$V_{rms}^2 = \int_0^\infty g^2(\omega) v_{rms}^2(\omega) d\omega = \frac{\omega^2 \tau^2}{(1 + \omega^2 \tau^2)^2} \frac{eI_{in}}{\pi \omega^2 C^2} d\omega = \frac{eI_{in} \tau}{4C^2}$$

The input rms charge squared necessary to produce a signal equal to the rms noise output is obtained by setting  $V_{rms}^2$  equal to  $(0.37 Q_{rms}/C)^2$ , resulting in

$$Q_{rms}^2 = 1.8eI_{in} \tau \quad (\text{base and detector current noise})$$

The collector current noise (shot noise) may be represented by a current generator  $i_{rms}^2 = (eI_c \delta\omega)/\pi$  in parallel with the collector, or by a voltage generator of magnitude  $v_{rms}^2 = (r_e^2 e I_c \delta\omega)/\pi$  at the base. Following a similar procedure, we find

$$Q_{rms}^2 = (0.34 r_e^2 e I_c^2) / \tau \quad (\text{collector current shot noise})$$

where  $r_e$  is the emitter resistance and  $I_c$  is the collector current.

The base and detector leakage current noise squared is proportional to the amplifier time constant  $\tau$ , while the collector current (shot) noise squared is inversely proportional to  $\tau$ , and, in general, an optimum value of  $\tau$  results. Since the base and detector current noise is proportional to the current  $I_d + I_b$ , low leakage detectors (such as the guard ring detector) and low base leakage ( $I_{CBO}$ ) transistors are required for low noise. Since the collector current noise is proportional to the total input capacitance, the detector, base-emitter, and base-collector capacitances should be as small as possible.

In order to illustrate the results obtained above, noise versus amplifier time constant data were taken on an earlier developed low noise transistor amplifier based on the 2N930 transistor. The 2N930 satisfies the requirements for a low noise input stage. It has a  $\beta > 250$  at 10 microamperes collector current,  $f_\alpha \approx 150$  Mc,  $C_{bc} \approx 2$  pf, and  $I_{CBO} < 5 \times 10^{-9}$  amps. The circuit configuration is shown in Fig. 1. The data are presented in Fig. 2, where the full-width-at-half-maximum in Kev is plotted against the amplifier time constants in microseconds on a log-log scale. The shot noise contribution and base current noise contribution are clearly indicated.

The circuit schematic of the transistor cascode preamplifier is shown in Fig. 3. The preamplifier is composed of (a) a charge feedback input stage whose output is proportional to the energy deposited into the detector; (b) a feedback amplifier connected as a differentiator;

(c) a similar feedback amplifier connected as an integrator and (d) an emitter follower output stage. The differentiation and integration time constants are set to be 1 microsecond. This corresponding to a reasonable time constant for minimum noise even in the presence of appreciable detector leakage, which could conceivably develop.

The cascode charge loop is composed of transistors  $Q_1$ ,  $Q_2$ ,  $Q_3$ , and  $Q_4$  (See Fig. 4). The transistors  $Q_1$  and  $Q_2$  form the input cascode circuit. The cascode configuration gives a minimum of Miller capacitance at the input and provides a configuration to obtain a large open loop gain with a minimum of phase shift. Transistors  $Q_3$  and  $Q_4$  are connected in a transistor version of the White cathode follower used in vacuum tube circuits. This modified emitter follower is used to bootstrap the load resistors  $R_{10}$  of  $Q_2$ , drive the feedback capacitor  $C_8$  and provide a low source impedance to drive the voltage gain stage  $Q_5$  and  $Q_6$ . The open loop gain of this cascode configuration is approximately  $(R_{e8}/r_{e2}) \approx 1000$  where  $R_{e8} = [R_7/(1-A_{Q3Q4})]$  in parallel with the collector resistance  $r_c$  of  $Q_2$ , and  $r_{e2}$  is the emitter resistance of  $Q_2$ . An approximation of the value of  $r_{e2}$  is given by  $[(25.6 \times 10^3)/I_e] \approx 1000$  ohms. For a large open loop gain, the closed loop gain is controlled by the ratio of the feedback capacitor  $C_8$  and the input capacitance. Under these conditions, the output voltage of the charge loop is  $Q_0/C_8$  or approximately 20mv/Mev where  $Q_0$  is the charge produced in the detector by a nuclear particle. The modified emitter follower  $Q_3$ ,  $Q_4$ , is used because it provides higher input impedance, lower output impedance, and higher gain than a single emitter follower. The two feedback loops  $Q_5$ ,  $Q_6$  and  $Q_7$  and  $Q_8$ , utilize an npn pnp direct coupled pair. Feedback is from the collector of the output transistor to the emitter of the input transistor providing the required degenerative path. In the first feedback pair, the gain is set to a nominal value of 40 by  $R_{23}$  and  $R_{20}$ . However, the resistor  $R_{22}$  is bypassed by a capacitor  $C_{13}$  which is too small to provide appreciable bypassing at low frequencies. In the feedback loop this effectively behaves as a differentiator providing an extremely low

gain at low frequencies and increasing gain up to the full gain at high frequencies. When the reactance of  $C_{13}$  is comparable to  $R_{20}$  the gain is halved thus these two components control the time constant which is fixed at  $.01 \times 10^{-6}$  farads  $\times 100$  ohm = 1 microsecond.  $Q_7$  and  $Q_8$  function in a similar fashion to provide the integrating time constant.  $R_{31}$  and  $R_{28}$  provide a nominal gain of 10. The resistor  $R_{30}$  is sufficiently bypassed that it plays no role in the feedback path. However,  $C_{18}$ , serves to provide increased feedback at high frequencies. When the reactance of  $C_{18}$  becomes comparable to  $R_{31}$ , the gain will be reduced by 3 db. These two elements then provide the controlling time constant of  $100 \times 10^{-12}$  farads  $\times 10^4$  ohms = 1 microsecond.  $Q_9$  is the output emitter follower capable of furnishing reasonable currents to the external circuit while the standby power is kept low. The precise values of the feedback resistor  $R_{23}$  is selected to fix the output sensitivity at 0.5 volts/Mev. A test capacitor  $C_4$  is provided to permit operating the amplifier on test pulses. An attenuator  $R_{34}$ ,  $R_2$ , provides a termination for the pulse generator and reduces the signal applied to the test capacitor  $C_4$  to a level sufficient to avoid spurious pick-up from being coupled in on the test input lead. The amplifier (Fig.5) is constructed in the form of a modified cordwood structure. By that is meant the components are stacked cordwood fashion between two circuit boards which carry the interconnections between the components. Four such stacks are employed. The first containing  $Q_1$  and  $Q_2$  and the input circuit components, the second  $Q_3$  and  $Q_4$ . The third  $Q_5$  and  $Q_6$  and the fourth  $Q_7$ ,  $Q_8$  and  $Q_9$ . Power and signal leads are used to connect the four stacks together forming a rigid structure capable of functioning in environments involving high vibration and shock. The rigid structure is necessary not only for environmental reasons but to preserve the precise relationship between the critical parts of the input circuit which determine the calibration factor of the instrument. The over-all dimensions of the amplifier are such that it fits snugly into a  $1/2" \times 2" \times 3"$  drawn metal can which serves as a shield against external pick-up fields. The input is in the form of a standard transistor socket projecting from one end of the can. While the amplifier is normally constructed with a connec-

tor for power and output signal, for the proton dosimeter pigtail type leads are used to conserve space.

3. Threshold Circuit - As has been discussed earlier, it is necessary to impose a threshold on the amplifier output in order to avoid integrating noise and minimum ionizing pulses. At the same time however, the presence of this threshold should not affect the linearity or precision of the integrated proton pulses. A number of threshold circuits have been studied and shown to be satisfactory. However, from the point of view of simplicity, low power consumption and high reliability, the simple transistor energy gap type of circuit was adopted. This is shown in Fig.6.  $Q_1$  the input transistor, fixes the threshold. This is a silicon planar transistor which has a base energy gap of approximately 0.6 volts. That is to say, its base is essentially reverse biased until the input signal level reaches positive 0.6 volts. When this level is exceeded, the input signal minus the energy gap appears at the emitter through the feedback action of the conventional emitter follower connection. At the same time, current flows in the collector circuit which turns on the pnp transistor  $Q_2$  which has previously been biased off by  $R_2$ . For signals exceeding the threshold of a few millivolts,  $Q_2$  is saturated due to the cascaded current gain of  $Q_1$  and  $Q_2$ . The saturating of  $Q_2$  results in approximately 2 milliamperes being conducted through diode  $D_1$ . This provides a step at the anode of diode  $D_1$  of approximately 0.6 volts. This step is used to compensate for the 0.6 volt lost from the input pulse by the threshold circuit. In addition, a gating signal indicating that a pulse is to be integrated, is present at the anode of  $Q_2$  and is used for switching the integrator. Performance of the threshold circuit is as predicted. The isolation for signals less than threshold is approximately 1000 i.e. a sub-threshold signal is attenuated by approximately a factor of 1000 in  $Q_1$ . This isolation is limited primarily by the capacitance between the base and emitter of  $Q_1$ . This capacitance grows increasingly large as the threshold is approached and reaches approximately 5pf for just sub-threshold signals. To avoid integration on such sub-threshold

signals, additional isolation will be required.

4. Integrator Circuit - The purpose of the integrator circuit is to act effectively as an inverse charge amplifier, that is a voltage pulse corresponding to a given charge deposited into the detector is converted by this circuit into a charge deposited in the electrochemical cell. The requirements on the integrator circuit are rather severe. In addition to performing the voltage charge conversion, it must include provision for unidirectional excitation of the E-cell. By unidirectional excitation is meant that the negative overshoot which accompanies the input pulse must not be permitted to flow through the cell. Since the area of the overshoot is precisely equal of pulse, there would be no net integration. Thus, a rectifier must be included in the integrator circuit to permit integration of only one polarity signal. While an ideal rectifier should introduce no difficulty, most actual rectifiers are quite non-linear in the vicinity of zero input. This non-linearity is characterized generally by an energy gap and a square law region of response and it is clearly undesirable that such a response be imposed on the integrator. So for this reason means must be employed to eliminate the non-linearity of the rectifier. An additional requirement on the integrator is the ability to gate the integration signal without the introduction of spurious signals. This requirement for gating comes from the inherent feedthrough of the threshold circuit. The integrator circuit is shown in Fig.6 utilizing  $Q_3$  and  $Q_4$ .  $Q_4$  serves basically as an operational amplifier in which currents from  $C_2$  and  $C_3$  and from the feedback path including the E-cell are summed in the base circuit. The base can be viewed as a current node since  $Q_4$  is chosen for extremely high  $\beta$ . If a pulse is applied to  $C_2$  and  $C_3$ , these capacitors can charge only by current flowing into the base node. This current must be supplied by the E-cell feedback loop, the amount of charge for example that will flow through this loop is clearly  $C_2 \times V$  of the input pulse and the charge which will flow to charge  $C_3$  is  $C_3 \times$  voltage present at the anode of  $V_1$ . This current note approach effectively provides the inverse charge amplifier action, i.e. the charge through the E-cell circuit is exactly

proportional to the voltage of the pulsed signal. Diodes  $D_2$  and  $D_3$  serve a dual function. Their primary function is to act as the rectifier for the E-cell. During the pulse itself,  $D_2$  conducts, routing the feedback current through the E-cell. During the overshoot, diode  $D_3$  conducts and diode  $D_2$  opens thus providing a bypass path for the feedback current around the E-cell during the overshoot. In addition, the energy gap of diodes  $D_2$  and  $D_3$  serve to effectively isolate the E-cell from the circuit unless the signal communicated by  $C_4$  exceeds the energy gap of these diodes approximately 0.6 volts.  $Q_3$  acts as a clamp to prevent a signal of this magnitude appearing at the collector of  $Q_4$  unless it is desired to integrate. Resistor  $R_8$  from the base of  $Q_3$  to ground effectively places  $Q_3$  in saturation. Its saturation resistance is well under 10 ohms. Therefore, any signal that is developed across  $Q_3$  will be equal to the current through  $Q_4 \times 10$  ohms. Clearly such signals will be extremely small and in practice are very much smaller than the energy gap of diode  $D_2$  and  $D_3$ . Thus the combination of the shunt gate  $Q_3$  and the series gate formed by  $D_2$  provides an isolation of greater than  $10^6$  for noise signals, which may feed through the threshold circuit. This combined with the isolation of  $10^3$  of the threshold circuit, produces an over-all isolation of  $10^9$  greatly in excess of anything that might possibly be required. When integration is desirable,  $Q_3$  is cut off by the gating pulse conducted through  $C_1$ . This is a positive going pulse from the threshold circuit and is more than adequate to completely cut off  $Q_3$ . The load resistor or  $Q_4$  is then only the feedback circuit, and since any current going in the feedback circuit over and above that required to charge the input capacitors  $C_2$  and  $C_3$  would cut off  $Q_4$ , the effective gating transients is essentially eliminated. Thus all of the requirements for the integrator circuit are fulfilled. The size of  $C_2$  and  $C_3$  is chosen in such a way as to provide the calibration factor for the system. These two capacitors are nominally equal for precise compensation of the bias introduced by the threshold circuit. A slight adjustment of  $C_3$  relative to  $C_2$  can be made to compensate for

any imbalance between the diode gap of  $D_1$  and the input gap of  $Q_1$ . In practice, the effect on the over-all integrated result can be neglected and these capacitors chosen with moderate tolerances. The threshold and integrator circuit is build into an additional cordwood module similar to those making up the amplifier. The E-cell is located externally for convenience. The closed circuit phone jack is used to connect and disconnect the E-cell from the circuit and to permit its being readout by means of external currents. A jack is also provided at the input for monitoring the pulse signals at the input to the threshold circuit.

5. Power Supply Requirements - While maximum effort has not been made to minimize the power consumption, the over-all power requirements are quite moderate. The amplifier and threshold integrator circuits require approximately 5 milliamperes at 22 volts. This is approximately 110 milliwatts which should not impose serious power problems except for self-contained battery operation. Such self-contained operation is clearly desirable in the case of the operational use of the device. This would permit complete freedom of movement of the astronaut during the period in which dose was being accumulated without the necessity of obtaining power from a central source. In a laboratory prototype, the self-contained power supply is extremely convenient for acquiring data in connection with accelerators since the use of long power cables in accelerator experiemtns is an invitation to difficulties with ground loops and pick up. It is clearly desirable to use a re-chargeable battery since power will be available from the central power supply for re-charging as required. In the laboratory prototype, two nickel cadmium cells Burgess type CZ-28, were used. These provide almost 80 hours of continuous operation of the dosimeter between charge. They are however, quite bulky and heavy contributing approximately 8 cu.in. to the over-all dimensions of the instrument. However, for laboratory prototype purposes, it is adequate. Future operational instruments can reduce this requirement in one of three ways:
- (1) Reduction in the over-all power consumption of the amplifier which can easily be accomplished by appropriate design efforts.
  - (2) The use of different types of batteries such as the silver cadmium type.

(3) The reduction in the amount of capacity between charges.

In addition to the main power consumption, approximately 100 volts is required to bias the detector. This is essentially a shelf life type of service for batteries, the drain being of the order of 1 microampere. For the laboratory prototype, six 22.5 volt carbon zing cell stacks were used. Future instruments for operational purposes will derive this bias from the main power supply by means of a small DC to DC converter. With an efficiency of only 10%, this would contribute only 50 microamperes to the total drain.

6. Readout Circuit - The integrated information which is contained in the form of plated silver in the E-cell is most conveniently readout by measuring the amount of charge required to plate the silver back on another electrode. If this plating is accomplished by means of a constant current, then the time required for complete plating is a measure of the integrated dose. Now a wide variety of instruments could be used for readout in actual operational situations. A laboratory readout instrument was constructed to permit evaluating the dosimeter and to provide a convenient means of calibration. Fig.7 is a schematic diagram of the laboratory readout system which was constructed. The constant readout current is provided by a zener diode and one of two resistors which are switch selectable. The readout currents used are approximately 10 microamperes and 40 microamperes for the x1 and x4 positions respectively. During plating the cell voltage does not exceed 50 millivolts such that the input transistor whose base is connected across the E-cell will be cut off. When the end point is reached, the cell essentially becomes an open circuit and the plating current is then switched to the base of the input transistor. This transistor rapidly goes into conduction and its collector bottoms to ground. The collector of the input transistor is connected to an emitter follower which controls the operation of the relaxation oscillator. The relaxation oscillator is a unijunction transistor type 2N2646 with the period determined by a 10 microfarad and two 100K resistors. If the emitter follower is turned on, then the 10 microfarad capacitor charges through the top 100K resistor and the base of Q<sub>3</sub>. When the firing point for the emitter of the unijunction is reached, the 10 microfarad capacitor then discharges through the

unijunction and the lower 100K resistor back biasing  $Q_3$  and turning it off. The collector of  $Q_3$  is directly coupled to the base of  $Q_4$  which drives the mechanical register. By this means, the mechanical register advances at the rate of 1 count every 0.1 second as long as the plating process continues. The over-all calibration factor is fixed in such a way that each register count corresponds very closely to 1 MR.

7. Calibration and Results - Dosimetry system and readout has been extensively calibrated utilizing pulse generator pulses,  $\alpha$  particles and thin window detectors and 30 Mev protons incident on the actual detector. Fig.8 shows the integrated dose versus input for a wide variety of pulse rates and amplitudes. The extreme linearity within experimental error will be noted down to the threshold pulse height. At the threshold pulse height, the integrated output drops rapidly to zero. Calibration points with  $\alpha$  particles and with 30 Mev protons from the USC linear accelerator, are noted on this figure.

## XI. SUMMARY

The prototype instrument has been developed for measuring proton dose in space. The detector is a 2x2x2mm lithium ion drift detector immersed in a matrix of tissue equivalent material and sealed in a TOS transistor can. An all transistor preamplifier and integrator circuit is used to indicate dose in the form of metal plated in an electrochemical cell. A prototype readout circuit is provided to permit reading out of the cell. Pulse generator calibration and preliminary calibration with  $\alpha$  particles and protons, confirms the linearity and dynamic range of the system. Adaptation to the operational requirements of the Apollo program include:

- (1) Miniaturization of the electronics to approximately 1 cu.in.
- (2) Reduction of power consumption from approximately 100 milliwatts to approximately 20 milliwatts.
- (3) Adaptation of the readout system to an operationally suitable means of indication.
- (4) Calibration against acceptable absolute standards with a wide variety of proton energies.



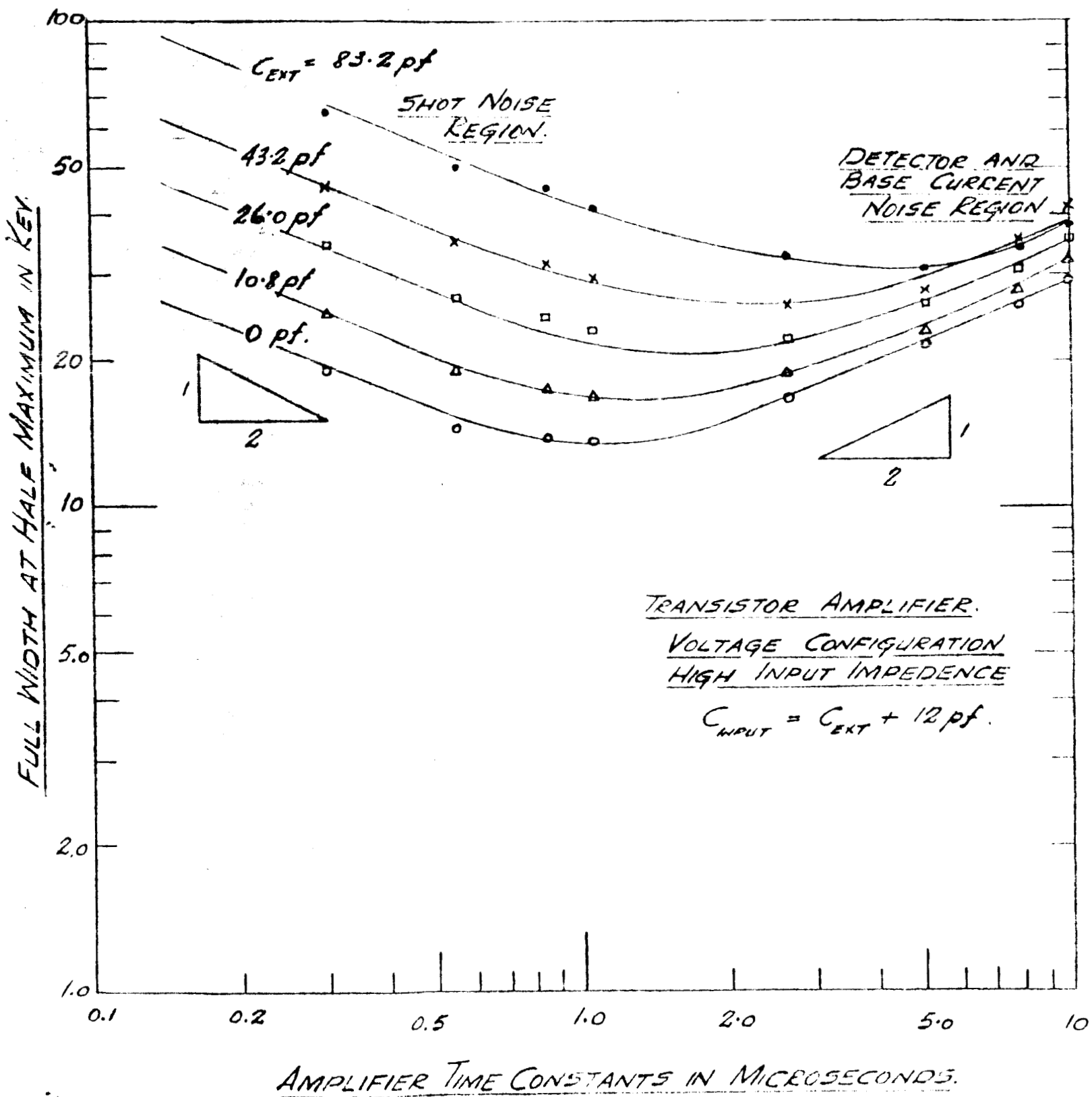


Fig. 2

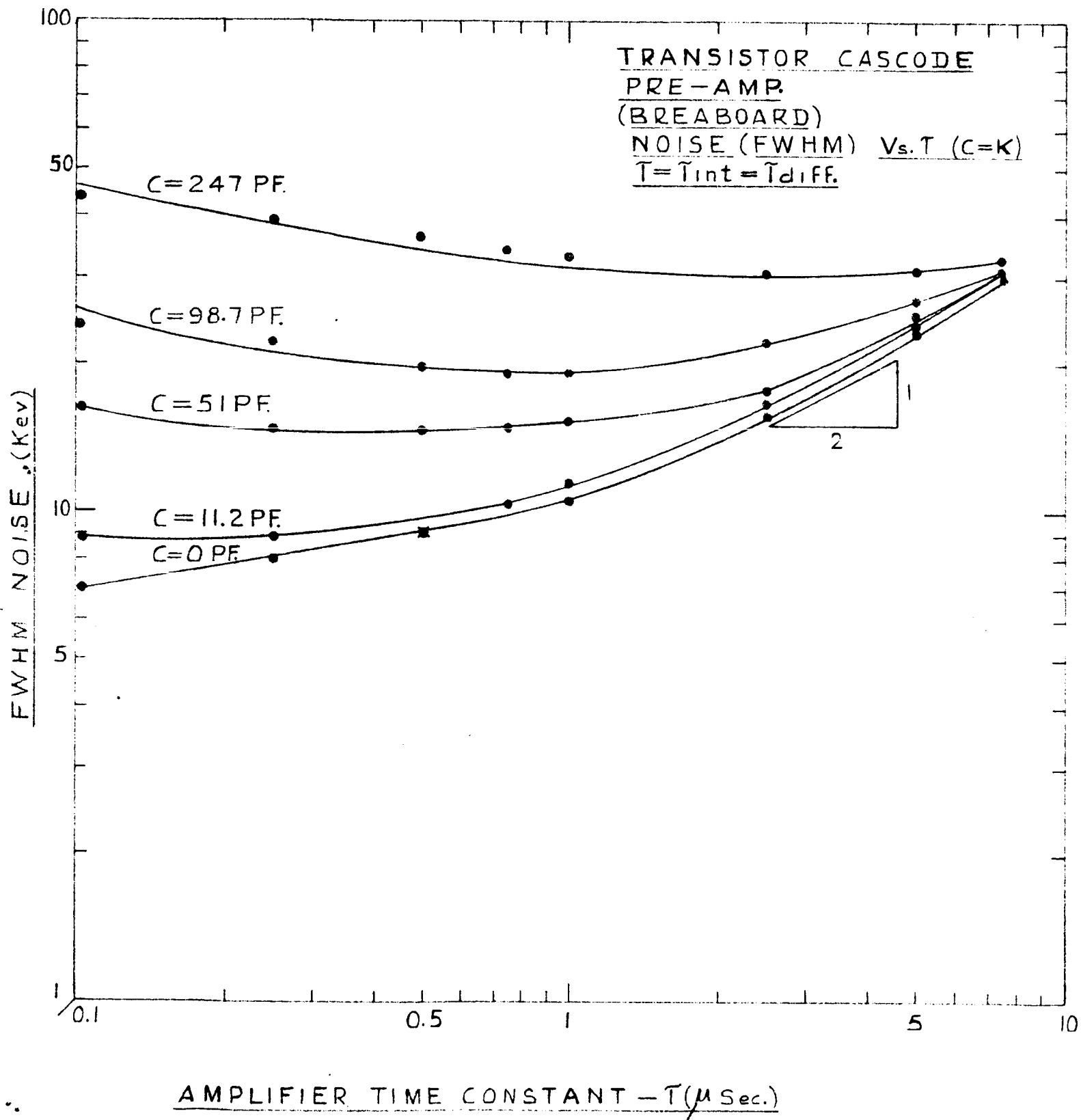
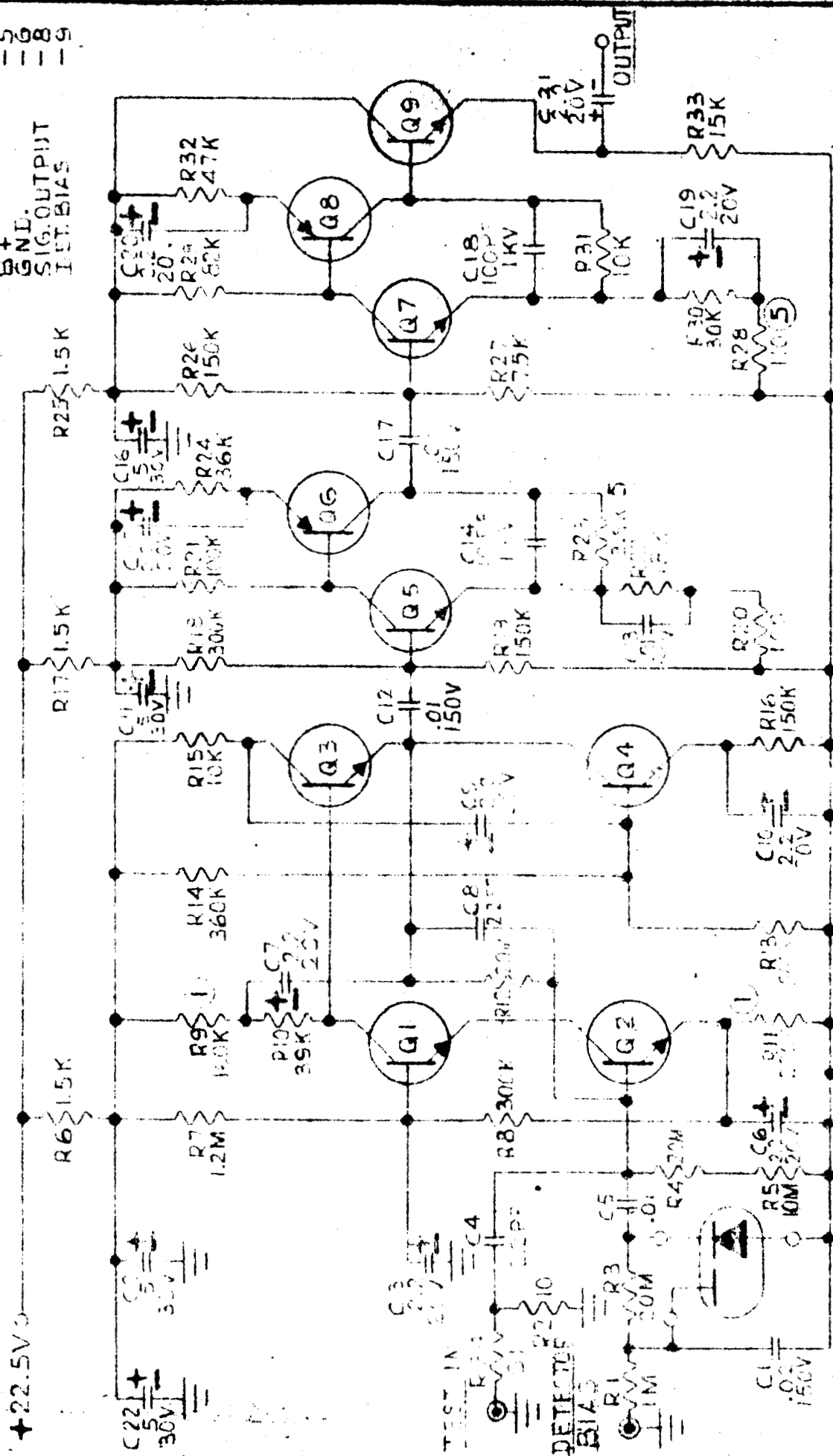


Fig. 4

RE-9P CANNON  
TEST INPUT  
-1-5-8-9  
GND.  
SIG. OUTPUT  
DET. BIAS



# NOTES:

1. ADJUST FOR INPUT CURRENT
2. Q1, Q2, Q3, Q4, Q5, Q6, Q7, Q8, Q9: 2N934; Q10: 2N918
3. ALL RESISTORS IN OHMS
4. ALL CAPACITORS IN MFD UNLESS OTHERWISE NOTED
5. ADJUST FOR DESIRED GAIN

RECORDS  
LIST OF MATERIALS

NASA  
V. B. S. 8-108  
RECEIVED

MODEL 108  
CASCODE PRE-AMP  
1453-32

FIG 5

+0 22.5V

R9  
1K

R2 10K

R6 220K

C1 .001

R5 1K

R4 10K

R8 10K

C4

C2 .005

C3 .005

R7 16K

R10 2K

C5

R3 1K

R1 10K

D1

D3

C6

D2

+ 30V  
C7 5

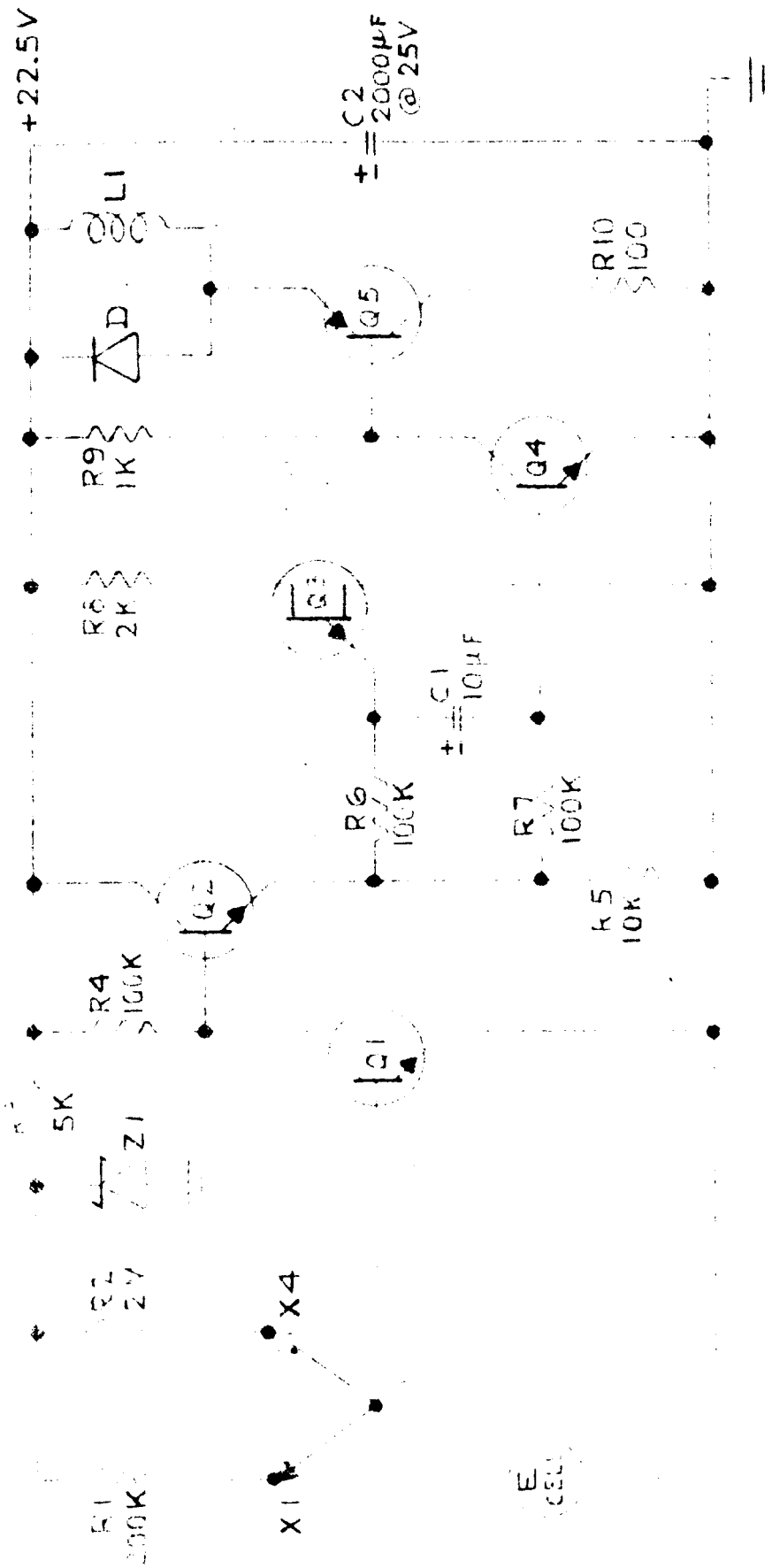
FROM  
108  
OUTPUT

# NOTES

1. ALL CAPACITORS IN MICROFARAD
2. ALL RESISTORS IN OHMS. 1/4W. 5%
3. D1, D2, D3 - 1N919
4. Q1, Q4 - 2N2716; Q2, Q3 - 2N869

MILITARY MATERIAL	
SOLID STATE RADIATION INC.	
2001 S. 10TH ST. SUITE 100	
DENVER, CO 80202	
DOSIMETER INTEGRATOR	
1554-26	

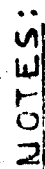
Fig. 6



NOTES:

1. ALL CAPACITORS IN MICROFARADS
2. ALL RESISTORS IN OHMS
3. Q1, Q2, Q3, Q4, Q5 - 2N1646
4. Z1 - 18V
5. D - IN207
6. LI - VEEFLEX NOCT COUNTER

SOLID STATE RADIATIONS, INC.	
1000 N. 10TH AVE. SUITE 100	
DENVER, COLORADO 80202	
PROTON DOSE SCALER	
1554-27	



- |     |            |             |                           |
|-----|------------|-------------|---------------------------|
| Q53 | DATE REC'D | DATE FORW'D | Q54                       |
|     |            |             | NAME: V. B. R. 100-64     |
|     |            |             | ADDRESS:                  |
|     |            |             | CITY: CHICAGO, ILL. 60606 |
|     |            |             | STATE: ILL. ZIP: 60606    |
|     |            |             | TELEPHONE: (312) 462-1111 |
|     |            |             | CLASS: 100-64             |
|     |            |             | REMARKS: 100-64           |
|     |            |             | 1554-27                   |

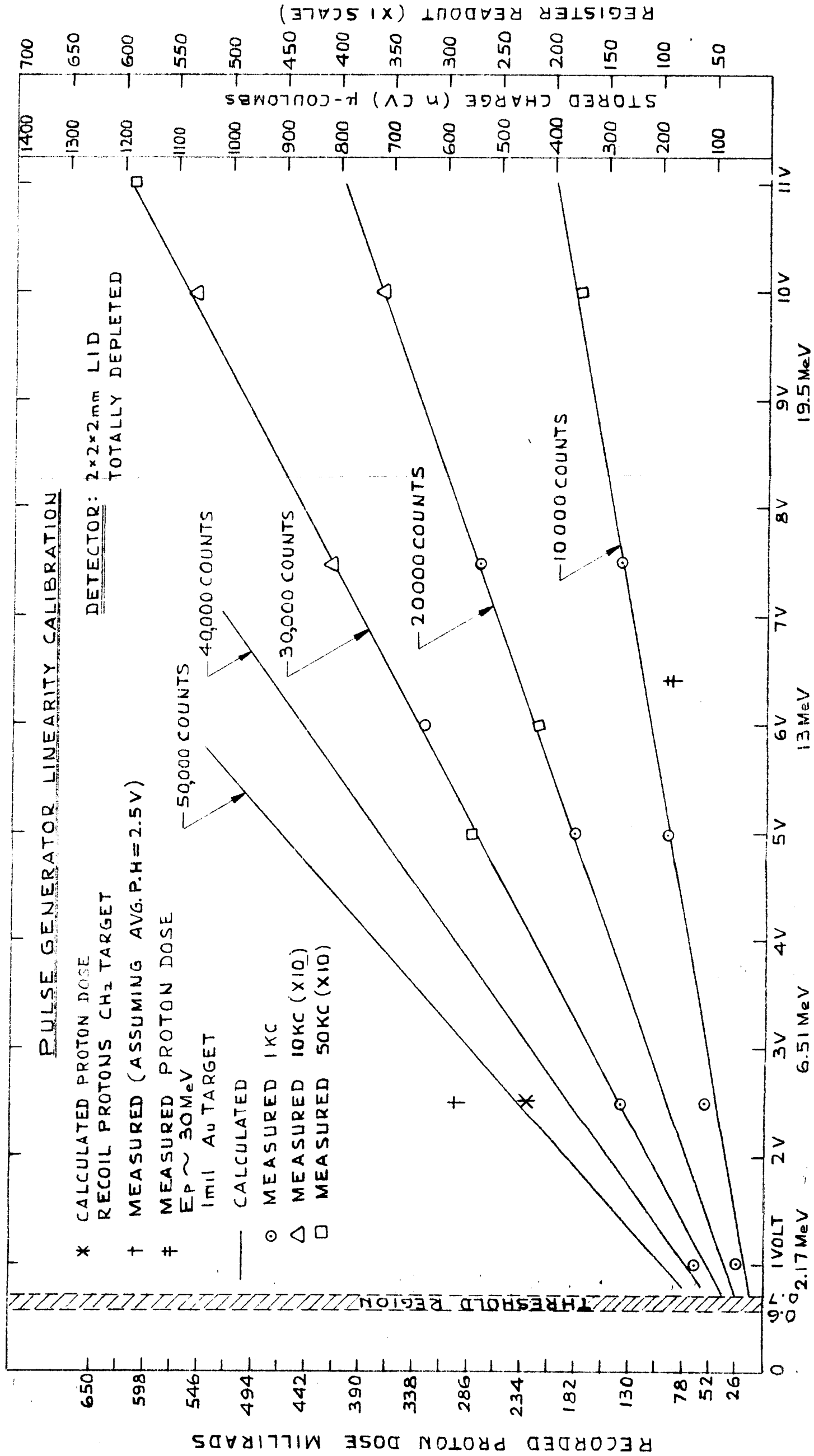


FIG. 8